

# Three-Axis Autopilot Design for a High Angle-Of-Attack Missile Using Mixed $H_2/H_\infty$ Control

**Dae-Yeon Won\*** and **Min-Jea Tahk\*\***

*Department of Aerospace Engineering, Korea Advanced Institute of Science and Technology, Daejeon 305-701, Korea*

**Yoon-Hwan Kim\*\*\***

*LIG Nex1 Co., Daejeon 305-345, Korea*

## Abstract

We report on the design of a three-axis missile autopilot using multi-objective control synthesis via linear matrix inequality techniques. This autopilot design guarantees  $H_2/H_\infty$  performance criteria for a set of finite linear models. These models are linearized at different aerodynamic roll angle conditions over the flight envelope to capture uncertainties that occur in the high-angle-of-attack regime. Simulation results are presented for different aerodynamic roll angle variations and show that the performance of the controller is very satisfactory.

**Key words:** Mixed  $H_2/H_\infty$  control, Three-axis autopilot, Linear matrix inequality technique

## 1. Introduction

The increased demand for high maneuverability of modern missiles requires excellent autopilot performance over a large flight envelope. The main difficulty in missile autopilot design is the influence of high angle-of-attack aerodynamic phenomena on stability characteristics (Hemsch, 1992). As a missile executes a high angle-of-attack maneuver, the forebody vortices can become asymmetric and give rise to significant lateral-forces and yawing moments. Classically, missile autopilots are designed using gain scheduling approaches in roll, pitch, and yaw channels (Blakelock, 1991; Shamma and Athans, 1992; Shamma and Cloutier, 1993; White et al., 2007). However, the performance of single-axis autopilot design approaches are limited within some flight boundaries because aerodynamic coupling effects and their parameter dependencies in large angle-of-attack aerodynamics could not be considered. In this context, the design of a three-axis missile autopilot has been studied using linear and nonlinear control approaches (Choi et al., 2008; Devaud et al., 2001; Kim et al., 2008). These methods are

based on gain scheduling techniques by local linearization, and demonstrate some improvements from a practical point of view.

In this paper, a three-axis missile autopilot design with a multi-objective output-feedback control theory is presented. Because high angle-of-attack aerodynamics is highly nonlinear and estimates of the aerodynamic coefficients are very imprecise, a mix of  $H_\infty$  and  $H_2$  criteria is employed to guarantee the performance of the three-axis missile autopilot. This control methodology, which uses linear matrix inequality (LMI) techniques, was motivated by the work in (Schere et al., 1997).

This paper is organized as follows. In Section 2, we give an overview of multi-objective output-feedback control theory. Section 3 describes our formulation of the missile control problem. Section 4 describes strategies and numerical simulation results for the designed autopilot. Our conclusions are provided in Section 5.

© \*Graduate Student  
\*\*Professor

\*\*\* Senior Research Engineer, Corresponding author,  
E-mail: mjtahk@fdcl.kaist.ac.kr;  
Tel: +82-42-350-3718; Fax: +82-42-350-3710

## 2. Multi-Objective Control

This section gives a brief overview of multi-objective output-feedback synthesis via the LMI approach described in (Chilali and Gahinet, 1996; Gahinet and Apkarian, 1994). For the missile autopilot design problem, the control objectives include  $H_\infty$  and  $H_2$  performance.  $H_\infty$  performance is a convenient way to enforce robustness and model uncertainty with frequency domain specifications.  $H_2$  performance is a useful way to address the output power (or error) of a generalized system due to unit intensity white noise input.

Consider a generalized plant with

$$\begin{aligned} \dot{x} &= Ax + B_1\omega + B_2u \\ z &= C_1x + D_{11}\omega + D_{12}u \\ y &= C_2x + D_{21}\omega + D_{22}u \end{aligned} \quad (1)$$

where  $A \in \mathbf{R}^{mn}$ ,  $D_{12} \in \mathbf{R}^{p1 \times m2}$ , and  $D_{21} \in \mathbf{R}^{p2 \times m1}$ . In addition,  $x$ ,  $u$ ,  $z$ ,  $y$ , and  $w$  are the state, control input, controlled output, measurement output, and exogenous input, respectively. The multi-objective control problem is to find an LTI control law  $u = K(s)y$  that minimizes an upper bound for the  $H_2$  gain subject to an  $H_\infty$  gain constraint.

### 2.1 Multi-Objective LMI Formulation

The LTI controller  $K(s)$  can be represented in state-space form by

$$\begin{aligned} \dot{x}_K(t) &= A_K x_K(t) + B_K y(t) \\ u(t) &= C_K x_K(t) + D_K y(t) \end{aligned} \quad (2)$$

For the LMI approach to multi-objective synthesis, nonlinear terms added in the output feedback case should be eliminated by an appropriate change of controller variables. This change of controller variables is implicitly defined in terms of the Lyapunov matrix  $P$  as follows:

$$P = \begin{bmatrix} Y & N \\ N^T & V \end{bmatrix}, P^{-1} = \begin{bmatrix} X & M \\ M^T & U \end{bmatrix} \quad (3)$$

The new controller variables can be written as

$$\begin{cases} \hat{A}_K := NA_K M^T + NB_K C_2 X + YBC_K M^T \\ \quad + Y(A + B_2 D_K C_2)X, \\ \hat{B}_K := NB_K + YB_2 D_K, \\ \hat{C}_K := C_K M^T + D_K C_2 X, \\ \hat{D}_K := D_K \end{cases} \quad (4)$$

The mixed  $H_2/H_\infty$  synthesis would then involve finding  $X$ ,  $Y$ , and new controller variables such that Eqs. (5-9) hold while minimizing  $\gamma$  and  $\nu$ :

$$\begin{bmatrix} \Psi_{11} & \Psi_{21}^T & \Psi_{31}^T & \Psi_{41}^T \\ \Psi_{21} & \Psi_{22} & \Psi_{32}^T & \Psi_{42}^T \\ \Psi_{31} & \Psi_{32} & \Psi_{33} & \Psi_{43}^T \\ \Psi_{41} & \Psi_{42} & \Psi_{43} & \Psi_{44} \end{bmatrix} < 0 \quad (5)$$

$$\begin{bmatrix} \Gamma_{11} & \Gamma_{21}^T & \Gamma_{31}^T \\ \Gamma_{21} & \Gamma_{22} & \Gamma_{32}^T \\ \Gamma_{31} & \Gamma_{32} & \Gamma_{33} \end{bmatrix} < 0 \quad (6)$$

$$\begin{bmatrix} X & I & * \\ I & Y & * \\ C_1 X + D_{12} \hat{C}_K & C_1 + D_{12} \hat{D}_K C_2 & Q \end{bmatrix} > 0 \quad (7)$$

$$\text{Tr}(Q) < \nu \quad (8)$$

$$D_{11} + D_{12} \hat{D}_K D_{21} = 0 \quad (9)$$

with the shorthand notation

$$\begin{aligned} \Psi_{11} &:= AX + XA^T + B\hat{C}_K + (B\hat{C}_K)^T \\ \Psi_{21} &:= \hat{A}_K + (A + B_2 \hat{D}_K C_2)^T \\ \Psi_{22} &:= A^T Y + YA + \hat{B}_K C_2 + (\hat{B}_K C_2)^T \\ \Psi_{31} &:= (B_1 + B_2 \hat{D}_K D_{21})^T \\ \Psi_{32} &:= (YB_1 + \hat{B}_K D_{21})^T \\ \Psi_{33} &:= -\gamma I \end{aligned} \quad (10)$$

$$\begin{aligned} \Psi_{41} &:= C_1 X + D_{12} \hat{C}_K \\ \Psi_{42} &:= C_1 + D_{12} \hat{D}_K C_2 \\ \Psi_{43} &:= D_{11} + D_{12} \hat{D}_K D_{21} \\ \Psi_{44} &:= -\gamma I \\ \Gamma_{11} &:= AX + XA^T + B_2 \hat{C}_K + (B_2 \hat{C}_K)^T \\ \Gamma_{21} &:= \hat{A}_K + (A + B_2 \hat{D}_K C_2)^T \\ \Gamma_{22} &:= A^T Y + YA + \hat{B}_K C_2 + (\hat{B}_K C_2)^T \\ \Gamma_{31} &:= (B_1 + B_2 \hat{D}_K D_{21})^T \\ \Gamma_{32} &:= (YB_1 + \hat{B}_K D_{21})^T \\ \Gamma_{33} &:= -I \end{aligned} \quad (11)$$

### 2.2 Controller Computations

Note that the multi-objective output-feedback synthesis is an LMI problem of the form

$$\begin{aligned} &\text{Minimize } \gamma + \nu \text{ over } X, Y, \hat{A}_K, \hat{B}_K, \hat{C}_K, \hat{D}_K, \gamma, \nu \\ &\text{satisfying Eqs. (5-9)} \end{aligned} \quad (12)$$

After solving the synthesis LMIs, the controller computation proceeds as follows:

- Find a nonsingular matrix  $M$ ,  $N$  to satisfy  $MN^T = I - XY$  via SVD.

- Solve the linear equation (Eq. 4) for the controller  $K(s)$  by computing (Eq. 13).

$$\begin{cases} D_K := \hat{D}_K, \\ C_K := (\hat{C}_K - D_K C_2 X) M^{-T}, \\ B_K := N^{-1} (\hat{B}_K - Y B_2 D_K), \\ A_K := N^{-1} (\hat{A}_K - N B_K C_2 X - Y B_2 C_K M^T \\ \quad - Y (A + B_2 D_K C_2) X) M^{-T} \end{cases} \quad (13)$$

This LMI optimization problem can be efficiently solved with the LMI Control Toolbox (Gahinet et al., 1995). The solution of the LMI problem gives us an upper estimate of the suboptimal  $H_\infty$  and  $H_2$  performance.

### 3. Missile Control Problem Formulation

#### 3.1 Missile Model and Autopilot Requirements

We considered a three-axis nonlinear missile model of a skid-to-turn cruciform missile with a high angle-of-attack. Sensors and actuator modeling were also taken into account. We assumed that the missile plant had 5 degrees of freedom (DOFs) with the fixed altitude and longitudinal velocity. Also, rigid body dynamics was considered. Under these assumptions, the 5-DOF rigid body equations of motion were expressed using differential equations describing the translational motion and rotational motion as follows:

$$\begin{aligned} \dot{v} &= -ru_0 + pw + F_y / m \\ \dot{w} &= -pv + qu_0 + F_x / m \\ \dot{p} &= L / I_{zz} \\ \dot{q} &= -(I_{xx} - I_{zz}) / I_{yy} pr + M / I_{yy} \\ \dot{r} &= -(I_{yy} - I_{xx}) / I_{zz} pq + N / I_{zz} \end{aligned} \quad (14)$$

where  $(u, v, w)$  are the longitudinal, lateral, and vertical body velocities,  $(p, q, r)$  are the roll, pitch, and yaw body rates,  $(I_{xx}, I_{yy}, I_{zz})$  are the inertial moments,  $(F_x, F_y)$  are the external forces, and  $(L, M, N)$  are the external moments. For the missile plant, the external forces and moments are produced by aerodynamics forces and nonlinear functions of the angle-of-attack, bank angle, and deflection angles. The actuator was modeled using a second-order transfer function between the commanded fin deflection and the actual fin deflection:

$$\frac{\delta}{\delta_{cmd}} = \frac{\omega_{act}^2}{s^2 + 2\zeta_{act}\omega_{act}s + \omega_{act}^2} \quad (15)$$

where  $\delta$ ,  $\delta^{cmd}$ ,  $\omega_{act}$ , and  $\zeta_{act}$  are the actual fin deflection, commanded fin deflection, natural frequency, and damping coefficient, respectively. The state-space form of the missile

model is written as

$$\begin{aligned} \dot{x}_m &= A_m x_m + B_m u_m \\ y_m &= C_m x_m + D_m u_m \end{aligned} \quad (16)$$

where

$$\begin{aligned} x_m &= \{\alpha, q, \beta, r, p, \phi, \delta_z, \dot{\delta}_z, \delta_y, \dot{\delta}_y, \delta_r, \dot{\delta}_r\}^T \\ y_m &= \{\eta_z, q, \eta_y, r, \phi, p\}^T \\ u_m &= \{\delta_{zc}, \delta_{yc}, \delta_{rc}\}^T \end{aligned} \quad (17)$$

In this expression,  $\alpha$ ,  $\beta$ , and  $\phi$  are the angle of attack, side-slip angle, and bank angle, respectively;  $\delta_z$ ,  $\delta_y$ , and  $\delta_r$  are the actual tail deflections in the pitch, yaw, and roll axes, respectively; and  $\eta_z$  and  $\eta_y$  are pitch and yaw acceleration commands, respectively. The inputs to the missile plant are commanded tail deflections  $\delta_{zc}$ ,  $\delta_{yc}$ , and  $\delta_{rc}$ . Therefore, the accelerations, bank angle, and angular rates are available for feedback. The total incidence angle  $\alpha' = \arccos(\cos\alpha \cos\beta)$  was used for scheduling, but the aerodynamic roll angle  $\phi' = \arctan(\tan\beta \sin\alpha)$  was not measurable in this missile problem.

The aim of the proposed autopilot design is to steer the missile to track the acceleration guidance commands generated by an outer loop and stabilize the missile airframe at a given bank angle. The stabilization of the bank angle is a critical requirement for controlling a highly maneuverable missile. However, the aerodynamic roll angle is not measurable in a practical context. To deal with this problem, we found a dynamic controller  $K(s)$  to satisfy the given multi-objective for the multi-model using LMI techniques.

#### 3.2 Interconnected System Model

The performance specifications for the closed-loop system in terms of multi-objective control are as follows:

- Guarantee an upper bound on the L2-induced gain  $\gamma$  of the operator mapping  $z$  to  $\omega$ .
- Minimize an upper bound on the variance of  $z_2$  due to the disturbance  $\omega$ .

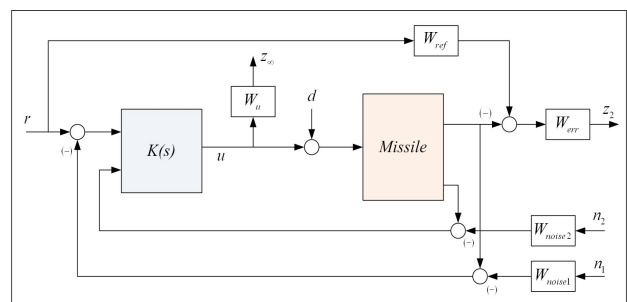


Fig. 1. Control structure and interconnection for missile plant.

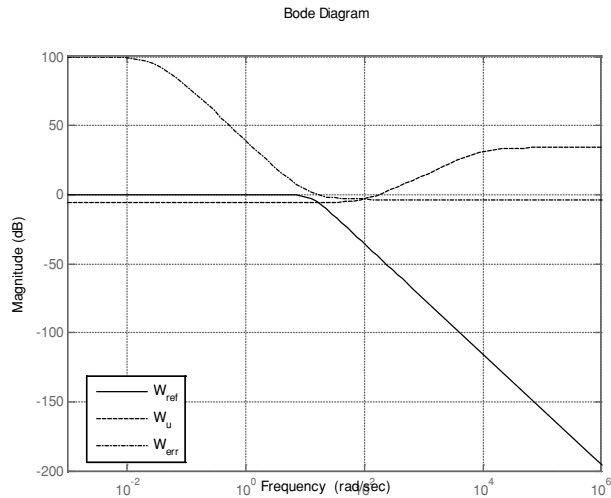


Fig. 2. Frequency responses of the weighting function.

These performance requirements of the closed-loop system were transformed into the multi-objective control framework with weighting functions. Weight functions were selected to account for the relative magnitudes of signals, frequency dependence, and relative importance. This method allows the controller designer to apply classical loop-shaping concepts to obtain good performance while optimizing the response near the system bandwidth to achieve robust stabilization. The continuous time synthesis plant  $P(s)$  was readily obtained from the connections shown in Fig. 1, and incorporated in the missile model  $G(s)$  and weighting functions  $W_{ref}$ ,  $W_{err}$ , and  $W_u$ . These frequency-dependent weights were tuned by performing a few synthesis and simulation trial-and-error iterations on  $s$  for the nominal plant. Figure 2 shows the frequency responses of the weighting functions.

#### 4. Simulation Results

The angle-of-attack  $\alpha$  and the side-slip angle  $\beta$  were not available by measurement only. In this missile control problem,  $\alpha'$  and  $\phi'$  can capture the nonlinearities of the missile plant during a high angle-of-attack maneuver. However,  $\phi'$  is not available for scheduling while  $\alpha'$  can be estimated. Modern missiles suffer from variations in aerodynamic roll angle because of their extended flight regimes. Thus, an autopilot should be robust against aerodynamic roll angle variations. In this section, we present our simulation results for the three-axis missile autopilot design using LMI techniques.

Linear time-invariant (LTI) models of a nonlinear missile plant were derived at three fixed operating points. Table 1 shows the trim conditions of each operating point.  $V_t$  is the total velocity of the plant. The multi-model includes Model<sub>a</sub>, Model<sub>b</sub>, and Model<sub>c</sub>. Since LMI constraints can incorporate multiple models with the design criteria, we can formulate the proposed autopilot design strategy systematically.

Table 1. Trim conditions for local linearization

Model	Model <sub>a</sub>	Model <sub>b</sub>	Model <sub>c</sub>
$\phi'$	0.0°	22.5°	45°
$\alpha'$	15.4°	15.4°	15.4°
Vt	680.6 m/s	680.6 m/s	680.6 m/s

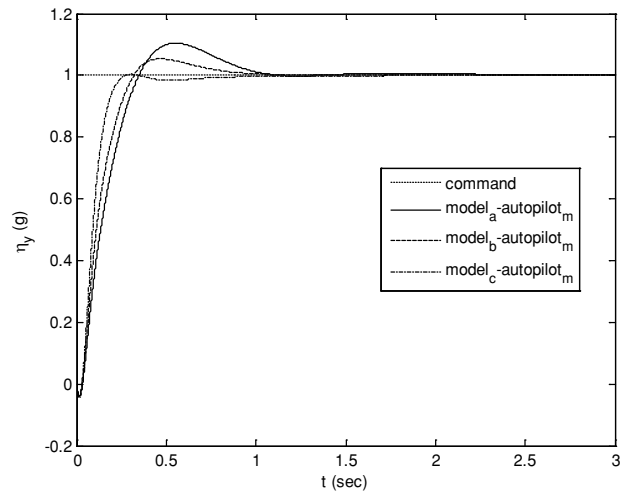


Fig. 3. Pitch acceleration step responses.

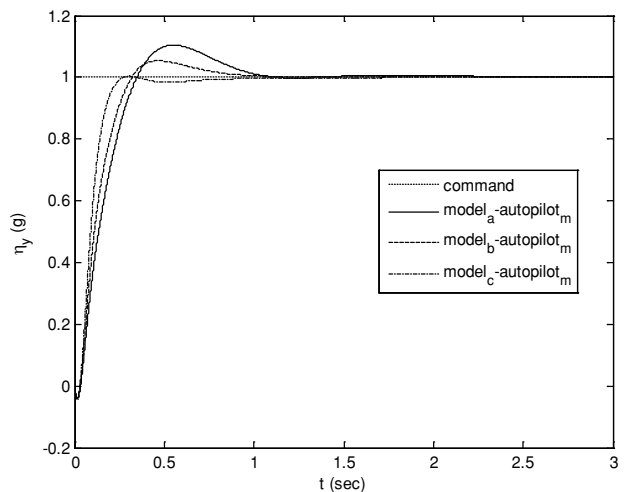


Fig. 4. Yaw acceleration step responses.

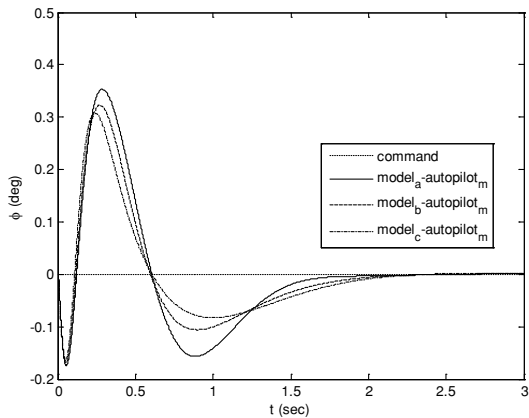


Fig. 5. Bank angle stabilization.

Figures 3-5 show the tracking performance of the proposed scheme. Notice that the autopilot guarantees  $H_2/H_\infty$  performance criteria for multiple linear models linearized at the different aerodynamic roll angle conditions. From the simulations results, we note that the performance goals were satisfied for each linearized model. However, the proposed controller cannot guarantee multi-objective performance for the entire flight trajectory in spite of its robustness. To overcome this conservativeness problem, studies of aerodynamic model uncertainties in the missile plant and additional linearized models for a wide range of aerodynamic roll angles are needed.

## 5. Conclusions

We proposed a three-axis missile autopilot design with multi-objective control synthesis. Our simulation results for the missile plant demonstrate the effectiveness and performance of the proposed control strategy in spite of its limitations. The results show that the designed autopilot provided satisfactory performance for nonlinearities over high angle-of-attack flight boundaries and uncertainties in the aerodynamic roll angle estimation.

## Acknowledgments

This research was sponsored in part by the Agency for

Defense Development in Korea under grant number ADD-09-01-03-03.

## References

- Blakelock, J. H. (1991). *Automatic Control of Aircraft and Missiles*. 2nd ed. New York: Wiley.
- Chilali, M. and Gahinet, P. (1996).  $H(\infty)$  design with pole placement constraints: an LMI approach. *IEEE Transactions on Automatic Control*, 41, 358-367.
- Choi, B. H., Kang, S. H., Kim, H. J., Won, D. Y., Kim, Y. H., Jun, B. E., and Lee, J. I. (2008). Roll-pitch-yaw integrated  $H(\infty)$  controller synthesis for high angle-of-attack missiles. *KSAS International Journal*, 9, 66-75.
- Devaud, E., Harcaut, J. P., and Siguerdidjane, H. (2001). Three-axes missile autopilot design: From linear to nonlinear control strategies. *Journal of Guidance, Control, and Dynamics*, 24, 64-71.
- Gahinet, P. and Apkarian, P. (1994). Linear matrix inequality approach to  $H(\infty)$  control. *International Journal of Robust and Nonlinear Control*, 4, 421-448.
- Gahinet, P., Nemirovski, A., Laub, A. J., and Chilali, M. (1995). *The LMI Control Toolbox User's Guide*. The MathWorks, Inc.
- Hemsh, M. J. (1992). *Tactical Missile Aerodynamics: General Topics*. Washington, DC: American Institute of Aeronautics and Astronautics.
- Kim, Y. H., Won, D. Y., Kim, T. H., Tahk, M. J., Jun, B. E., Lee, J. I., and An, J. Y. (2008). Integrated roll-pitch-yaw autopilot design for missiles. *KSAS International Journal*, 9, 129-136.
- Schere, C., Gahinet, P., and Chilali, M. (1997). Multi-objective output-feedback control via LMI optimization. *IEEE Transactions on Automatic Control*, 42, 896-911.
- Shamma, J. S. and Athans, M. (1992). Gain scheduling: potential hazards and possible remedies. *IEEE Control Systems Magazine*, 12, 101-107.
- Shamma, J. S. and Cloutier, J. R. (1993). Gain-scheduled missile autopilot design using linear parameter varying transformations. *Journal of Guidance, Control, and Dynamics*, 16, 256-263.
- White, B. A., Bruyere, L., and Tsourdos, A. (2007). Missile autopilot design using quasi-LPV polynomial eigenstructure assignment. *IEEE Transactions on Aerospace and Electronic Systems*, 43, 1470-1483.